Brazilian Journal
of Chemical
Engineering

ISSN 0104-6632
Printed in Brazil
www.abeq.org.br/bjche

Vol. 33, No. 04, pp. 885 - 896, October - December, 2016
dx.doi.org/10.1590/0104-6632.20160334s20150348

INFLUENCE OF THE MODEL SCALE ON HYDRODYNAMIC SCALING IN CFB BOILERS

P. Mirek

Institute of Advanced Energy Technologies, Czestochowa University of Technology
Dąbrowskiego 69, 42-201 Częstochowa, Poland.
Phone: + 48 34 3250 933; Fax: + 48 34 3250 933
E-mail: pmirek@neo.pl

(Submitted: January 24, 2015 ; Revised: October 17, 2015 ; Accepted: November 4, 2015)

Abstract - The paper presents the results of experimental verification of the simplified set of scaling parameters for which the particle density as well as the cold model length scale may be chosen independently. The tests were carried out on two large scale 1/10 and 1/20 geometrically similar cold models of the Lagisza 966 MW_{th} supercritical CFB boiler. The proposed set of dimensionless quantities allowed the Lagisza 966 MW_{th} CFB boiler to be closely modeled by cold models. However, the agreement between the hot bed and cold model's suspension density distributions is better for the 1/10 scale cold model. That suggests that the choice of the scale of a cold model is not without effect on the macroscopic movements of solids in the riser. Moreover, the study shows that a simplification of the scaling laws which excludes the very important solid-to-gas density ratio can give acceptable results over a wide range of boiler loadings.
Keywords: Fluidization; Similitude; Modeling; Dimensionless numbers.

INTRODUCTION

The main environmental advantage of Circulated Fluidized Bed (CFB) technology is its ability to burn a diverse range of difficult low grade fuels of varying quality with low emissions of NO_x, low-cost sulfur capture during combustion in the furnace itself, as well as low CO and C_xH_y emissions due to turbulent conditions and good mixing (Nowak and Mirek, 2013). Although CFB boilers have been investigated extensively for a long time because of their undeniable advantages, it is still impractical to design and operate them based on theoretical models (Qi *et al*., 2008). Due to the complex flow behavior that characterizes gas-solid systems, a complete description of circulating fluidized bed hydrodynamics remains a challenging task (Detamore *et al*., 2001). In the absence of alternative methods, scaling rules developed over the last two decades proved to be a reasonable tool for the scale-up and scale-down of fluidization processes (Sierra *et al*., 2009). As has been noted by Horio (1996), there have been three different approaches to the scaling law of fluidized beds: classical dimensional analysis (e.g., Buckingham π-theorem), differential equations (or, more specifically, non-dimensionalization of the continuum equations that describe multiphase flows) and theoretical solutions and experimental correlations.

Taking into consideration the second approach and differential equations derived by Anderson and Jackson (1967), Glicksman and coworkers (1994) formulated the following set of dimensionless quantities describing the state of the full hydrodynamic similarity between two unlike CFB systems:

$$\frac{U_0^2}{gH}, \frac{\rho_p}{\rho_f}, \frac{U_0 d_p \rho_p}{\mu}, \frac{U_0 H \rho_f}{\mu}, \frac{\dot{G}_s}{\rho_p U_0}, \quad \varphi, PSD, \text{geometry} \tag{1}$$

All these groups, respectively, refer to the Froude

*To whom correspondence should be addressed

number Fr_H based on the gas superficial velocity U_0, the solid to gas density ratio, the particle Reynolds number Re_p, the Reynolds number Re_H based on the riser height, the dimensionless solids flux, the particle sphericity φ, the particle size distribution and finally the geometrical characteristics. In formulation of the dimensionless quantities in Eq. (1) a general assumption has been made that particle to particle and particle to wall coefficients of restitution and friction, electrostatic forces and cohesion can be neglected (van der Meer *et al*., 1999). As follows from the set of scaling relationships, Eq. (1), apart from the requirement for geometric similarity, particle sphericity and particle size distribution, there are eight parameters $(U_0, H, g, \rho_p, \rho_f, \mu, d_p, \dot{G}_s)$ of importance to flow in the combustion chamber of a CFB boiler. Five of the above eight parameters called dependent ones $(H, \rho_p, d_p, \dot{G}_s, U_0)$, cannot be chosen independently. Their values are the result of the scaling calculations. The remaining three parameters (ρ_f, μ, g) called independent ones, can be chosen independently. The full set of scaling parameters requires that the small-scale unit needs to be roughly 0.25 the size of a CFB boiler and operated with particles of a density of 3.82 ρ_p (where ρ_p denotes here the particle density in a boiler) (Glicksman, 2003). Therefore, in scaling experiments where the only aim is to reflect the macroscopic flow pattern and the conditions in the boiler's combustion chamber satisfy the relationship $Re_p \leq 15$ (van der Meer *et al*., 1999), the set of scaling groups can be reduced to the following form

$$\frac{U_0^2}{gD}, \frac{U_0}{u_{mf}}, \frac{\dot{G}_s}{\rho_p U_0}, \text{geometry}, \varphi, PSD \tag{2}$$

The use of the set of scaling relationships in Eq. (2) allows the reduction of the number of dependent parameters from five to three and the increase of the flexibility in the scaling process. Thanks to this, it is possible to choose independently the cold model size as well as of the density of the particles in the scale model. In practice, the existence of two independent parameters leads to a question about the influence of the scale of a cold model as well as the density of an inert material, on the macroscopic movements of solids and the riser solids hold-up by volume inside the combustion chamber of a CFB boiler.

The use of a particulate material of a density lower than that resulting from the set of scaling groups in Eq. (1) in scaling experiments has been the subject of studies by many authors (Horio, 1996; Leckner *et al*., 2011; Kolar and Leckner, 2006; Mirek, 2011; Glicksman *et al*., 1987; Glicksman *et al*., 1993). Those studies have shown that a wide range of particulate materials of densities ranging from 1410 to 8800 kg/m^3 can be used in scaling experiments (see Table 1).

Table1: Particulate materials and scale factors used in scaling experiments.

	Scaled model			References
	ρ_p, kg/m^3	d_p, μm	Scale factor	
Plastic	1410	144.5; 99.5	0.25; 0.0625	Glicksman *et al*. (1993)
	1440	136	-	Bricout and Louge (2004)
FCC	1500	67	-	Qi *et al*. (2008)
FCC Catalyst	1780	46.4	0.25	Horio (1996)
Sand	2368	125	0.17	Kolar and Leckner (2006)
	2710	461	-	Qi *et al*. (2008)
Glass beads	2500	71.4	0.05	Mirek (2011)
	2530	97	-	Bricout and Louge (2004)
	2558	81.6; 88.3; 112.3; 78.7	0.25; 0.0625	Glicksman *et al*. (1993)
Iron	7860	56	0.11	Leckner *et al*. (2011)
Steel	8027	46	0.11	Leckner *et al*. (2011)
	8097	200	0.25	Glicksman *et al*. (1987)
	7300	58; 49.5	0.25; 0.0625	Glicksman *et al*. (1993)
Bronze	8563	73.4; 69.5	0.17	Kolar and Leckner (2006)
	8800	60	0.11	Sterneus *et al*. (2002)

As has been reported by Kolar and Leckner (2006), the use of a particulate material of an arbitrary density is not without an effect on the quality of the scaling process. Measurements taken on a transparent 12 MW_{th} boiler model (of scale of 1/6) operating at Chalmers University have clearly shown that the use of bronze particles (ρ_p = 8563 kg/m^3, d_p = 73.4 μm, 69.5 μm) allows a better matching of the static pressure curves to be achieved, compared with sand particles (ρ_p = 2368 kg/m^3, d_p = 125 μm). A similar conclusion has been reported by Glicksman *et al*. (1993). Based on the results of the viscous limit scaling using different particle densities (glass particles: ρ_p = 2558 kg/m^3, d_p = 112.3 μm; plastic particles: ρ_p = 1410 kg/m^3, d_p = 144.5 μm; steel particles: ρ_p = 7300 kg/m^3, d_p = 57.7 μm), they found that the solid density profiles of the two hot and cold (the length ratio - 1/4 of the combustor) beds matched fairly well, especially for steel powder used as the inert material.

The second parameter, whose value can be theoretically assumed at an arbitrary level, is the cold model scale. It has been noted that when the full set of scaling parameters is used, a cold model of an atmospheric combustor has linear dimensions approximately one-quarter those of the combustor (Glicksman, 2003). Nevertheless, as follows from Table 1, a wide range of scale factors ranging from 0.05 to 0.17 have been used by many researchers in scaling experiments. Kolar and Leckner (2006) carried out the scaling experiments on a 1/6 scaled-down version of a 12 MW_{th} CFB boiler operating at Chalmers University. The authors did not comment on the choice of the cold model length scale but claim that it is not possible to match all the nine scaling parameters simultaneously between the boiler and the cold model. From their point of view, particle size distribution as well as fluidizing velocity play a significant role in matching all scaling requirements. The operational characteristics of a 1/9 scaled-down plastic model used by Sterneus *et al*. (2002) have been calculated based on the following set of dimensionless numbers:

$$\frac{U_0^2}{gL}, \frac{\rho_p}{\rho_f}, \frac{U_0}{u_{mf}}, \frac{L_1}{L_2}, \frac{\dot{G}_s}{\rho_p U_0}, \varphi, PSD \tag{3}$$

As with work carried out by Kolar and Leckner (2006), the authors did not comment on the choice of the cold model length scale, but treat it as an input parameter for calculation of all small-scale equivalents. As a consequence, the gas velocity in the scale model is lower and is equal to 1/3 of the boiler velocity (Sterneus *et al*., 2002). In the scaling experiments carried out by Glicksman *et al*. (1993), the operating conditions for a 1/16 cold model were calculated based on a simplified set of scaling relationships of the following form:

$$\frac{U_0^2}{gH}, \frac{U_0}{u_{mf}}, \frac{\rho_f}{\rho_p}, \frac{H}{D}, \frac{L_1}{L_2} \tag{4}$$

As follows from experimental studies, the simplified set of dimensionless parameters in Eq. (4) allowed the atmospheric CFB boiler Studsvik 2.5 MW_{th} (cross-section: 0.7×0.6 m) to be closely modeled by the 1/16 cold model. Moreover, as has been noted by Glicksman *et al*. (1993), the average solid fraction profiles between the 1/4 scale cold model and the 1/16 scale cold model are in excellent agreement. This means that the simplified set of parameters in Eq. (4), which includes the gas to solid density ratio, can give acceptable results over a wide range of particle densities and bed sizes, even when the cross-section of a cold model is as small as 0.044×0.037 m. In summary, there are two things that most of the above-mentioned works have in common:

- in modeling of circulating fluidized bed hydrodynamics using the simplified set of dimensionless parameters, the choice of a cold model's length scale smaller than 1/4 is made without giving any reason,
- in modeling of large scale hot combustors with relatively small cold models, the solid to gas density ratio, particle size distribution and the fluidizing velocity play a significant role.

However, this brings up two questions:

- are there any other simplified sets of scaling parameters, especially excluding the solid to gas density ratio, that allow a cold model to model the macroscopic flow pattern occurring in the atmospheric CFB boiler?
- how does the scale of the cold model influence the vertical distribution of the inert material flowing inside the combustion chamber?

The purpose of the present paper is experimental verification of the simplified set of scaling parameters for which the particle density as well as the cold model length scale may be chosen independently. The unique feature of the current effort is that the experimental investigation has been conducted on two large scale 1/10 and 1/20 geometrically similar cold models of the Lagisza 966 MW_{th} supercritical CFB boiler operating at the company TAURON Wytwarzanie SA - The Lagisza Power Plant, Poland. Of particular interest is the influence of the cold model length scale on the average solid fraction pro-

files between the Lagisza 966 MW_{th} CFB boiler and the 1/10 and the 1/20 scale cold models.

DESCRIPTION OF THE SIMPLIFIED SCALING LAWS

The use of three dimensionless groups for similarity between circulating fluidized beds is justified only for small Reynolds numbers (Re_d< 4) (Glicksman *et al*., 1993). In this case, the simplified set of scaling relationships can be written as follows:

$$\frac{U_0^2}{gD}, \frac{U_0}{u_{mf}}, \frac{\dot{G}_s}{\rho_p U_0} \tag{5}$$

As can be noted from the comparison of dimensionless groups in Eqs. (1) and (5), in the simplified set of Eq. (5) the density ratio ρ_p/ρ_f has been excluded. The exclusion of this group is only justified when the similarity between macroscopic flow fields is more important than the sizes of clusters. Given that for CFBs the terminal velocity is a more appropriate parameter than minimum fluidization velocity, the set Eq. (5) can be re-expressed in the form proposed by van der Meer *et al*. (1999):

$$\frac{U_0^2}{gD}, \frac{U_0}{u_t}, \frac{\dot{G}_s}{\rho_p U_0} \tag{6}$$

As the measurement of the external solids circulation flux $\dot{G}_s$ in the Lagisza 966 MW_{th} CFB boiler is very difficult to accomplish, it is alternatively assumed that the set of Equations (6) can be substituted with the set of the following form:

$$\frac{U_0 d_{32} \rho_f}{\mu}, \frac{U_0}{u_t}, \frac{d_{32}^3 \rho_f (\rho_p - \rho_f) g}{\mu^2}, \text{geometry}, \varphi, PSD \tag{7}$$

As can be easily noticed, the Froude number and the ratio $\dot{G}_s/(\rho_p U_0)$ in the set Eq. (6) have been substituted with the particle Reynolds number and the Archimedes number, respectively. Introducing the Archimedes number allows the direct determination of particle size on the scaling model and, as a consequence, the determination of the superficial velocity U_0 from the condition of equality of particle Reynolds numbers. Due to the fact that the Lagisza 966 MW_{th} CFB boiler operates within the viscous flow range (Re_p<15), in the set of criterial numbers in Eq. (7) the density ratio ρ_p/ρ_f was omitted. When determining the dimensionless terminal velocity of particles in the boiler, U^*, and the terminal velocity, u_t, the drag coefficient C_d was calculated using the relationship given by Cheng, (2009):

$$C_d = \frac{432}{d_*^3}\left(1 + 0.022 d_*^3\right)^{0.54} + 0.47\left(1 - e^{-0.15 d_*^{0.45}}\right) \tag{8}$$

where d_* refers to the dimensionless particle diameter, defined as follows:

$$d_* = d_{32}\left[\frac{\rho_f(\rho_p - \rho_f)g}{\mu^2}\right]^{1/3} \tag{9}$$

EXPERIMENTAL STUDY

Operational Tests - Lagisza 966 MW_{th} Supercritical CFB Boiler

A reference facility for the cold model studies was the Lagisza 966 MW_{th} supercritical CFB boiler operating at the company TAURON Wytwarzanie SA - The Lagisza Power Plant, Poland (Figure 1).

The size of the combustion chamber at the grid level is 27.6 m long and 5.3 m wide.The depth of the combustion chamber grows with increasing distance from the grid. At the height of 8.95 m, the combustion chamber widthis 10.6 m and does not change with a further increase of the distance from the grid. The total height of the combustion chamber is 48 m. During the tests, the boiler was fired with bituminous coal (Ziemowit coal mine, Poland) with properties given in Table 2.

The proximate analysis of the bituminous coal was carried out with the help of the LECO TruSpec CHNS analyzer in accordance with PN-G-04584 and PN-G-04571 Standards. The low heating value (LHV) of the bituminous coal was determined with the help of the C 2000 basic IKA calorimeter in accordance with Standard PN-81/G-04513. The moisture, volatile matter and the ash contents of the coal have been determined in accordance with PN-80/G-04511, PN-G-04516:1998 and PN-80/G-04512/Az1:2002 Standards. The inert material samples were taken from the dense combustion chamber region at the hight of 8.3 m from the grid. These samples contained the broadest particle diameters spectrum and have been used for further cold model studies.A detailed description of the sampling method can be found in (Mirek, Ziaja, 2011). The operational tests were carried out for steady boiler operation conditions under the loads and with the primary (PA) to secondary air (SA) ratios as shown in Table 3.

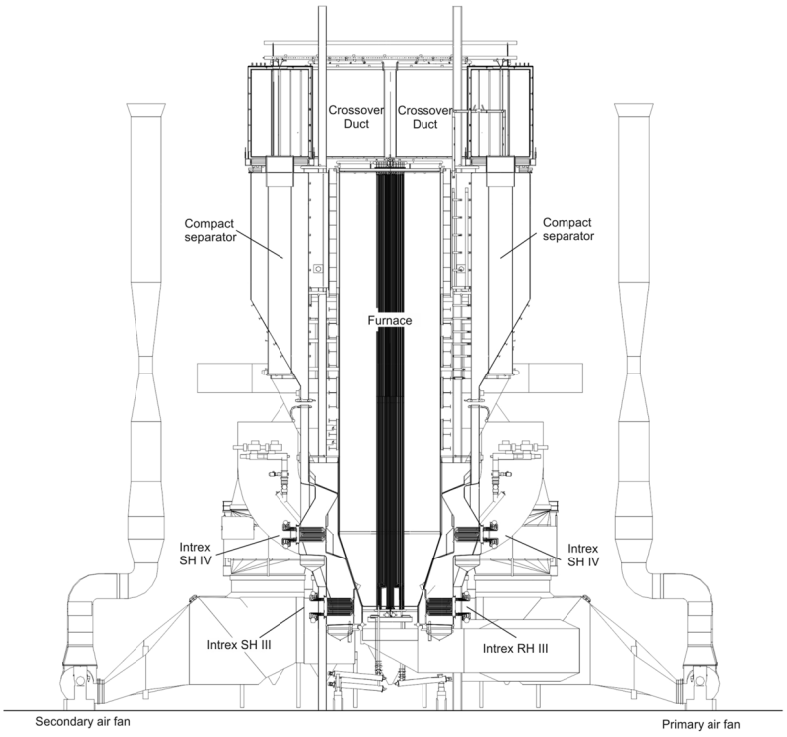

General		
Electric power	MW	460
Useful heat output	MW	966
Live steam		
Mass flow	kg/s	361
Pressure	MPa	27.5
Temperature	K	833
RH Steam		
Mass flow	kg/s	306
Pressure	MPa	5.48
Cold RH temperature	K	588
Hot RH temperature	K	853
Geometry		
Height	m	48
Cross-section of the combustion chamber (lower part)	m^2	146
Cross-section of the combustion chamber (upper part)	m^2	293

Figure 1: Schematic diagram of the Lagisza 966 MW_{th} supercritical CFB boiler.

Table 2: Proximate and ultimate analyses of bituminous coal.

Proximate analysis (as-received)			Ultimate analysis (air dried basis)		
Component	**Unit**	**Overall range**	**Component**	**Unit**	**Overall range**
C	wt, %	54.3-58.7	LHV	MJ/kg	21.35-23.48
$S^{combustible}$	wt, %	0.95-1.25	Moisture	wt, %	12.20-18.45
H	wt, %	3.93-4.15	Volatile matter	wt, %	26.55-29.72
N	wt, %	0.85-0.91	Ash	wt, %	10.42-18.17
$O^{bydifference}$	wt, %	7.82-8.81			

Table 3: Parameters of the Lagisza 966 MW_{th} CFB boiler and small-scale equivalents according to the set of simplified scaling laws Eq. (7).

		Lagisza SC-CFB				1/20 cold model				1/10 cold model			
MCR	.	100	80	60	40	100	80	60	40	100	80	60	40
U_0	m/s	5.10	4.17	3.14	2.62	1.49	1.22	0.92	0.76	1.49	1.22	0.92	0.76
PA/SA	-	1.86	2.33	3.00	5.25	1.86	2.33	3.00	5.25	1.86	2.33	3.00	5.25
d_{32}	m	$122.99 \cdot 10^{-6}$				$44.05 \cdot 10^{-6}$				$44.05 \cdot 10^{-6}$			
d_{50}	m	$234.57 \cdot 10^{-6}$				$84.01 \cdot 10^{-6}$				$84.01 \cdot 10^{-6}$			
ρ_p/ρ_f	-	8724				2076				2076			
μ	Pa s	$4.456 \cdot 10^{-5}$				$1.813 \cdot 10^{-5}$				$1.813 \cdot 10^{-5}$			
T	K	1123				293				293			
D	m	15.32				0.6				0.6			
u_t	m/s	0.479				0.139				0.139			
u_{mf}	m/s	0.00639				0.00187				0.00187			
Re_d	-	4.357	3.563	2.683	2.238	4.357	3.563	2.683	2.238	4.357	3.563	2.683	2.238
Ar	-	7.68				7.68				7.68			

MCR-Maximum Continuous Rating, %; U_0-superficial gas velocity, m/s; PA/SA-primary/secondary air ratio, -; d_{32}-Sauter mean particle diameter, m; d_{50}-mass mean particle diameter, m; ρ_p/ρ_f-particle/gas density ratio, -; μ gas viscosity, Pa s; T-temperature, K; D-riser hydraulic mean diameter, m; u_t-terminal velocity of particle, m/s; u_{mf}- minimum fluidization velocity, m/s

For the purpose of static pressure measurements along the combustion chamber height a measurement system was employed, which consisted of ADAM-6000 A/C converters, APR-2000ALW smart pressure sensors and DasyLab10.0 - data acquisition software.

Laboratory Tests - 1/20 and 1/10 Cold Models

Experimental tests were carried out on two 1/10 and 1/20 scale cold models of the Lagisza 966 MW_{th} supercritical CFB boiler. Because of the symmetrical design of the boiler, the 1/20 cold model was equipped with four cyclone separators and made up the half of the cross-section of the real boiler's combustion chamber (Figure 2).

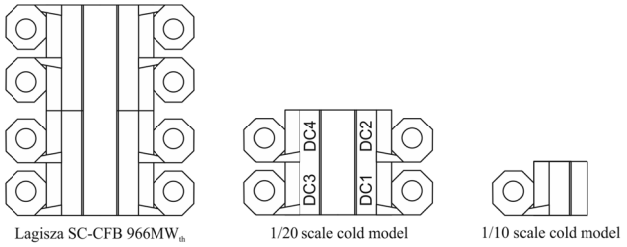

Figure 2: Cross-sections of the Lagisza 966 MW_{th} supercritical CFB boiler (27.6×10.6 m^2) and 1/20 (0.69×0.53 m^2; 1/2 of the Lagisza CFB boiler cross-section) and 1/10 (0.69×0.53 m^2; 1/8 of the Lagisza CFB boiler cross-section) scale cold models.

During the tests carried out on the 1/20 cold model the mass flow of solids was measured in four downcomers DC1, DC2, DC3 and DC4 of the test-stand (see Fig. 2). As follows from the results of the measurements presented in Figure 3, due to the symmetrical design of the 1/20 cold model its cyclone separators were loaded with an almost uniform mass flow of particulate material at all test-stand loads. This fact was the primary reason for building the 1/10 cold model equipped with a single cyclone separator. Here an additional assumption has been made, that for the purpose of macroscopic flow pattern studies the presence of the wall located in the symmetry axis of the real boiler does not significantly change the results of pressure measurements.

Based on mass flows of solids measured on the 1/20 cold model and relationship Eq. (10), it is possible to estimate the external solids circulation fluxes for different loads of the Lagisza 966 MW_{th} CFB boiler, depicted in Figure 4.

Figure 5 shows schematic diagrams of the 1/10 and 1/20 scale cold models made of plexiglass with the full geometrical similarity preserved. The cold models have identical 0.69 by 0.53 m cross-section.

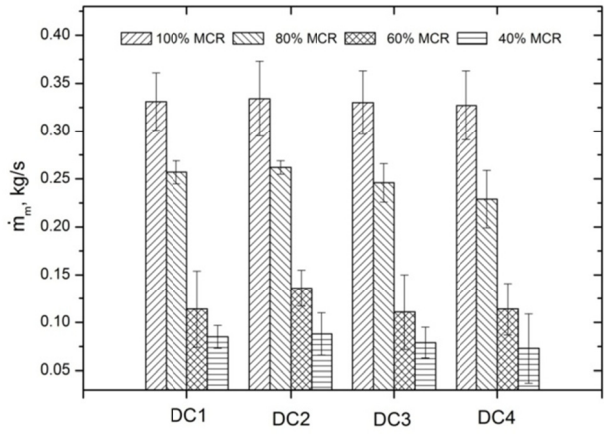

Figure 3: Mass flow of solids measured in downcomers DC1, DC2, DC3 and DC4 of the 1/20 cold model.

In order to relate the mass flows presented in Figure 3 to the mass flows occurring in the real boiler, the following relationship can be used

$$\dot{m}_b = \frac{U_{0b}}{U_{0m}} \frac{H_m}{H_b} \left(k_x k_y k_z\right)^{-1} \dot{m}_m \tag{10}$$

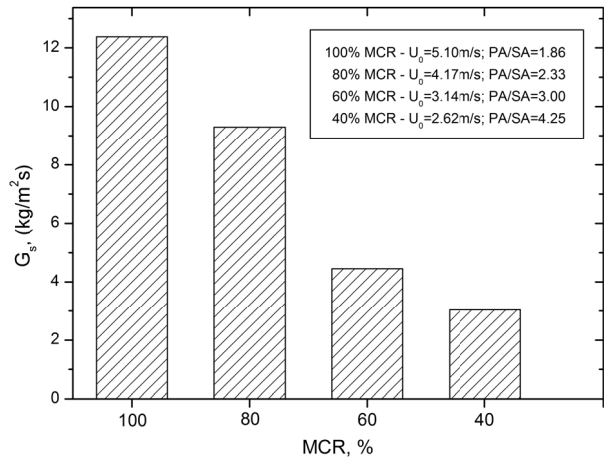

Figure 4: External solids circulation flux for different loads of the Lagisza 966 MW_{th} CFB boiler estimated based on tests carried-out on the 1/20 scaled-down model.

The test-stands are equipped with two independent compressed air systems, the first of which supplies the primary and secondary air channels, while the other delivers air to the Intrex separators and to the loop seals. The system of primary and secondary air is equipped with a radial industrial fan (2) of maximum capacity of 5500 m^3/h and a total pressure build-up of 20 kPa. For the other system, the source

of compressed air is the rotary screw compressor Aircenter 12SFC(7), with the following parameters: 74 m^3/h and 0.8 MPa. The fluidizing medium used in the tests was air with a density of 1.2 kg/m^3.The volumetric streams of the total, the primary and the secondary air were measured with the help of the measuring orifice plates K1-K4. Additionally, the PA stream was measured using a thermal sensor ST50. In pressure measurements, APR-2000 intelligent differential pressure transducers (5) with measuring ranges of ±2.5 kPa and ±10 kPa were used. The streams of air supplied to the Intrex separators and the loop seals were measured using rotameters (6). During the tests, static pressures along the combustion chamber height were recorded at ten measurement points corresponding to the measurement points located in the real boiler. In the 1/10 cold model the static pressure was measured via pressure taps located at distances scaled down from the boiler, viz: 3, 5, 8, 15, 22.5, 37.5, 66.5, 161.5, 275, 367 cm from the grid. In the 1/20 cold model the pressure taps were located at distances: 1.5, 2.5, 4, 7.5, 11.25, 18.7, 33.2, 80.7, 137.5, 183.5 cm from the grid. Depending on the boiler load, the fluidizing gas velocity was varied in the range of 0.76 - 1.49 m/s (see Table 2).

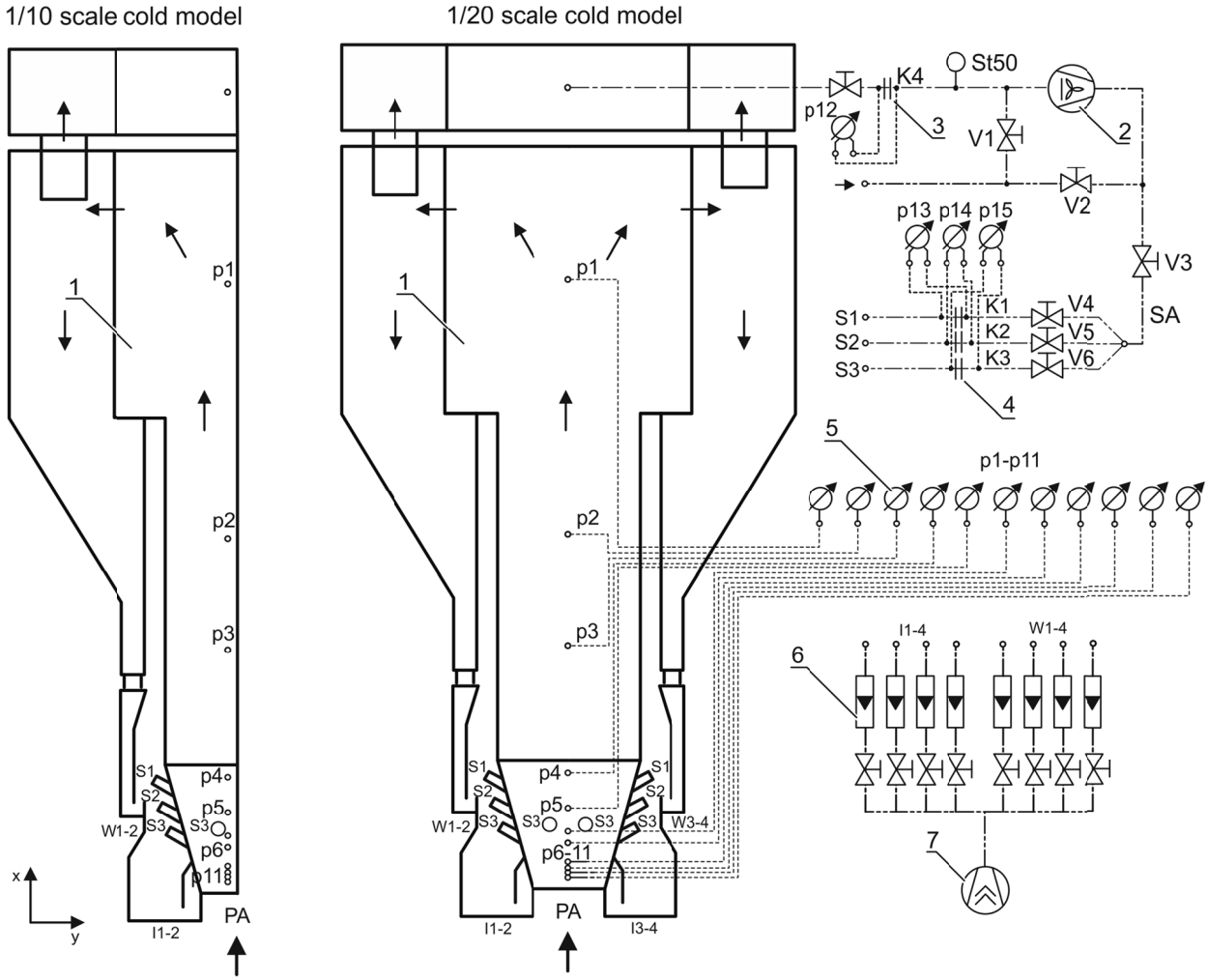

1-transparent model, 2-industrial radial fan of 5500m^3/h, p=20kPa, 3-measuring orifice plate for PA, 4-measuring orifice plates for three SA streams, 5-digital pressure sensors APR-2000ALW, 6-rotameters, 7-rotary screw compressor Aircenter 12SFC/0.8MPa, 74m^3/h, K1-K4-measuring orifice plates, S1-S3-SA sections, p1-p11-points of static pressure measurements in the riser, p12-p15-pressure drop measurements on orifice plates, I1-I4-Intrex air, W1-4-loop seal valve air, V1-V6-flap valves

Figure 5: The scaled-down models of the Lagisza 966 MW_{th} supercritical CFB boiler.

As a particulate material, quartz sand particles were used. The average density of the sand was determined in accordance with PN-Z-04002-01:1974 Standard and it was found to be 2500 kg/m^3. The average static porosity of the sand was determined in accordance with PN-Z-04002-02:1974 Standard and it was found to be 0.4. Figure 6 presents the scaled-down particle size distributions (PSD) of the boiler's inert material as well as inert material circulating in the Lagisza 966 MW$_{th}$ CFB boiler.

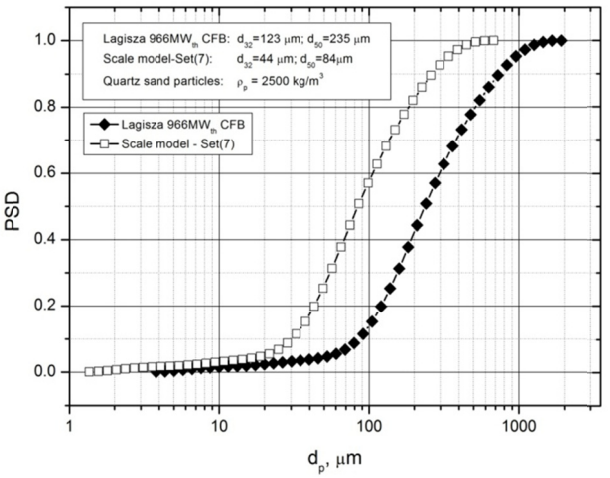

Figure 6: PSDs of the inert material circulating in the Lagisza 966 MW$_{th}$ CFB boiler and the scaling models calculated from the set of Eq. (7).

Depending on the boiler load, the tests were carried out with different fractions of primary and secondary air, whose streams could be controlled using flap valves V1-V6 (see Table 3).

EXPERIMENTAL RESULTS

Due to the fact that one of the primary parameters of CFB boilers is the particle volumetric concentration along the combustion chamber height, the results of experimental tests are represented in the form of the fluidized bed suspension density distribution. The following relation can be used to calculate the solids suspension density

$$\rho_b = \rho_p(1-\varepsilon) + \rho_f \varepsilon = -\frac{dp}{dh \cdot g} \tag{11}$$

The values of the suspended solids density have been presented in a dimensionless form and referred to the maximum value of this parameter. The error bars in the plots represent plus or minus the greater of the standard deviation of a number of solids suspension density measurements.

Figure 7 depicts a comparison of the dimensionless suspension density distributions determined for the Lagisza 966 MW$_{th}$ CFB boiler and 1/10 and 1/20 scale cold models for 100% MCR. As follows from the obtained distributions, the differences between values measured in the boiler's combustion chamber as well as the scale models are small. The exception is the bottom combustion chamber zone of the 1/20 scale cold model, where due to the very small distances between the static pressure taps p9-p11 (see Fig. 5) located in the close vicinity of the grid it was impossible to achieve reasonable values of the solids suspension density (Mirek, 2011). In the case of a bed with a low circulation rate, it constitutes the source of a significant error limiting pressure measurements for all test-stand loads within the range $0.04 \geq x/H \geq 1$.

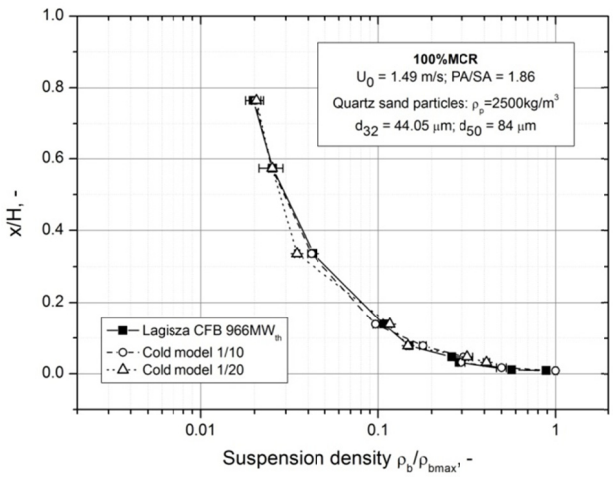

Figure 7: Suspension density distributions for the Lagisza 966 MW$_{th}$ CFB boiler and 1/10 and 1/20the scale cold models at 100% MCR.

Moreover, as indicated by the suspension density distribution obtained for the 1/20 scale cold model, the greatest differences from the values measured in the boiler's combustion chamber were recorded for x/H=0.03 (ca. 40%), x/H=0.05 (ca. 23%) and x/H=0.3 (ca. 19%). This implies that the level of deviation between the reference values and the values obtained in the model decreases with increasing distance from the air distributor. In the bottom part of the combustion chamber (x/H=0.03; x/H=0.05) the scatter of the solids suspension density values is the result of the intense turbulent mixing of particles and rapidly erupting bubbles, whose size in fluidized beds increases with gas velocity (Kunii and Levenspiel, 1991). In the dilute region (x/H=0.3), the reason for the lower pressure gradient is the influence of

the secondary air stream, which at the 100% MCR has the highest value compared to the primary air stream (PA/SA=1.86) and causes considerable dilution of the gas-solid mixture just above the supply region. With regard to the 1/10 cold model, the obtained suspension density distribution is in very good agreement with respect to the whole distribution registered in the boiler. Here, particular attention should be paid to the bottom part of the combustion chamber, where the greatest differences from the values measured in the boiler are only on the order of 11%.

Figure 8 shows a comparison of the dimensionless suspension density distributions determined for the Lagisza 966 MW_{th} CFB boiler and 1/10 and 1/20 scale cold models for 80% MCR. As indicated by the obtained distributions, better concurrence between values measured in the boiler's combustion chamber and in the cold models can be found for the 1/10 scale cold model. In relation to the 1/20 scale cold model the maximum deviation between the reference values and the values obtained in the model was found in the exit region (ca. 20%) and for x/H=0.14 (ca. 28%).

In the case of the 1/20 scale cold model the greatest difference from the values measured in the boiler's combustion chamber was recorded for x/H=0.03. In this part of the test-stand the solids suspension density differs by ca. 83% from the experimentally measured value in the Lagisza 966 MW_{th} CFB boiler. In the corresponding 1/10 scale cold model the solids suspension density differs by ca. 11% from the value registered in the boiler.

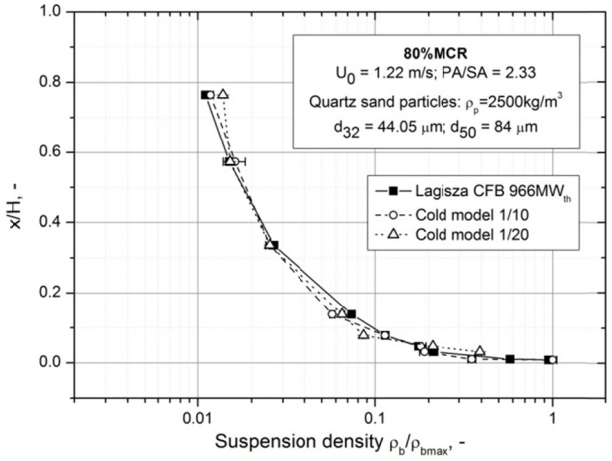

Figure 8: Suspension density distributions for the Lagisza 966 MW_{th} CFB boiler and the 1/10 and 1/20 scale cold models at 80% MCR.

Figure 9 shows a comparison of the dimensionless suspension density distributions determined for the Lagisza 966 MW_{th} CFB boiler and 1/10 and 1/20 scale cold models for 60% MCR. As can be seen from the obtained distributions, the differences between values measured in the boiler's combustion chamber and those measured on the scale cold models are again smaller for the 1/10 cold model.

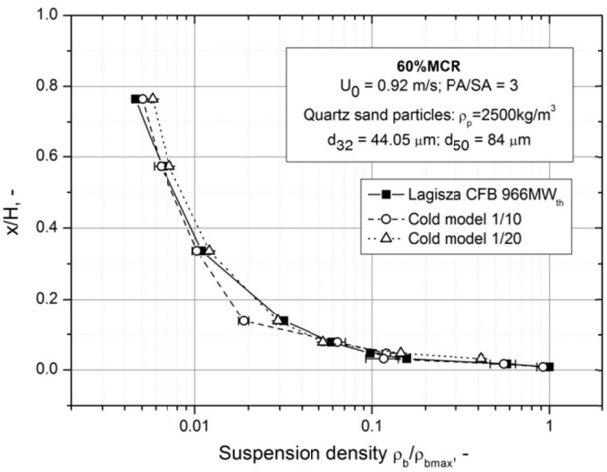

Figure 9: Suspension density distributions for the Lagisza 966 MW_{th} CFB boiler and the 1/10 and 1/20 scale cold models at 60% MCR.

The exception is the point at x/H=0.14 (the secondary air supply zone), where due to the smaller pressure drop the solids suspension density obtained from the model differs by ca. 67% from the existing experimentally measured value in the commercial unit. Since measurements were performed in the stable operating conditions (as evidenced by small lengths of the standard deviation bars), such a large discrepancy is quite puzzling and will be the subject of further studies. Taking into account the suspension density distribution measured in the 1/20 cold model the greatest differences from the values measured in the boiler's combustion chamber were recorded in the bottom part of the test-stand for x/H=0.03. In this place, the difference between values measured in the boiler and the cold-model is as high as 164%, but in the corresponding 1/10 scale cold model, the value of the solids suspension density differs by ca. 25% from the reference value.

Figure 10 shows a comparison of the dimensionless suspension density distributions determined for the Lagisza 966 MW_{th} CFB boiler and 1/10 and 1/20 scale cold models for 40% MCR. As indicated by the obtained distributions, the best consistency between values measured on the scale cold model and in the commercial unit was achieved for the 1/10 scale model. Nevertheless, as follows from the comparison of distributions presented in Figures 7-10 at this load, differences between values measured in the

boiler's combustion chamber and those in the 1/10 scale cold model are the greatest, especially in the bottom region (i.e., 111% for x/H=0.03).

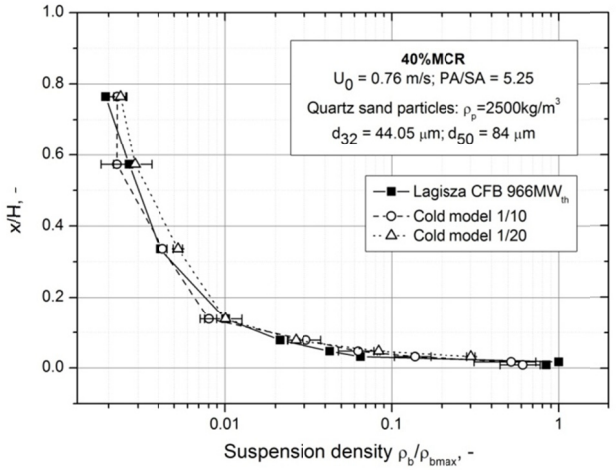

Figure 10: Suspension density distributions for the Lagisza 966 MW_{th} CFB boiler and the 1/10 and 1/20scale cold models at 40% MCR.

With regard to the 1/20 cold model, the corresponding value of solids suspension density differs by ca. 360% from the value measured in the Lagisza 966 MW_{th} CFB boiler. This implies that the bottom part of the cold model's combustion chamber exhibits very high sensitivity to variations in suspended solids density. As a consequence, an increase in the scatter of the results along with a decrease in the test-stands' loads can be observed. However, as has been demonstrated, this tendency is particularly noticeable for the smaller 1/20 cold model. As follows from the comparison of distributions presented in Figures 7-10, the higher the load of the test-stand, the higher the values of the solids suspension density. This state corresponds to the real operating conditions, where higher values of superficial velocity cause higher values of the solids suspension density along with the height of the boiler's combustion chamber. Moreover, as follows from the comparison between the solids suspension density distributions registered in the boiler and in the 1/10 scale cold model, the best fitting is attained for 100 and 80% MCR. A careful study of the suspension density profiles shows that the agreement between the 1/10 cold model and a hot bed is better near the exit region. The greatest differences from the values measured in the boiler's combustion chamber were recorded in the secondary air supply region for 60% MCR and the bottom zone for 40% MCR.

In summary, as follows from the distributions depicted in Figs. 7-10 the proposed set of simplified scaling parameters in Eq. (7), which excludes the very important the solid to gas density ratio, can give acceptable results over a wide range of boiler loadings operating in the viscous limit. However, the comparison between the distributions for the 1/10 and 1/20 scale cold models demonstrates that suspension density profiles measured on the bigger cold model are characterized by a better fit with respect to the distribution registered in the boiler. This implies that the scale of the cold model influences the vertical distribution of the inert material flowing in the riser. This conclusion is in contradiction to the experimental results obtained by Glicksman *et al.* (1993), however, who conducted their experiments on cold models having very small cross-sections (1/4 cold model - 0.16×0.16 m; 1/16 cold model - 0.044×0.037 m).

CONCLUSIONS

As has been demonstrated by the laboratory tests conducted:

1. The use of three dimensionless dynamic similarity numbers makes it possible to scale down hydrodynamics of the Lagisza 966 MW_{th} supercritical CFB boiler in the scale models with scale factors of 1/10 and 1/20.
2. Comparison between the distributions for the 1/10 and 1/20 scale cold models demonstrates that the agreement between the hot bed and cold models is better for the 1/10 scale cold model. This implies that the scale of the cold model influences the vertical distribution of the inert material flowing in the riser.
3. The 1/10 scale cold model allows the whole solids suspension density distribution registered in the boiler to be satisfactorily reflected in a scaling model. This was impossible in the 1/20 scale cold model, where, due to the very small distances between the static pressure taps located in the close vicinity of the grid, pressure measurements were significantly erroneous.
4. Decreasing the superficial velocity and, as a consequence, the load of the test-stands, results in an increase in scatter of the results, especially in the bottom part of the cold models. This trend is particularly noticeable for the smaller 1/20 cold model.
5. The level of deviation between the reference values of the solids suspension density and the values obtained in the cold models decreases with increasing distance from the air distributor.
6. The higher the load of the test-stand, the higher the values of the solids suspension density. This state corresponds to the real operating conditions, where

the higher values of superficial velocity cause higher values of solids suspension density along the height of the boiler's combustion chamber.

The use of the simplified set of scaling relationships in Eq. (7) allows an increase in flexibility in the scaling process. The number of dependent parameters can be reduced from five to three while maintaining the fluidization regime, macroscopic movements of solids and the distribution of solids suspension density along the height of the combustion chamber. Thanks to this, a large number of experiments can be performed for designing new CFB boilers and for modifying those whose performance can be improved. This requires, however, that the tests be carried out for small Reynolds numbers.

NOMENCLATURE

A	cross-sectional area (m^2)
Ar	Archimedes number $d_p^3\rho_f(\rho_p-\rho_f)g/\mu^2$ (-)
C_d	drag coefficient (-)
d_p	particle diameter (m)
d_*	dimensionless particle diameter (-)
d_{32}	Sauter mean particle diameter (m)
d_{50}	mass mean particle diameter (m)
D	riser hydraulic mean diameter $4A/P$ (m)
g	acceleration of gravity (m/s^2)
h	height (m)
H	combustion chamber height (m)
H_b	boiler's combustion chamber height (m)
H_m	cold model's combustion chamber height (m)
Fr_H	Froude number based on H $U_0^2/gH)$ (-)
$\dot{G}_s$	external solids circulation flux (kg/m^2s)
k_x, k_y, k_z	scale factor in x, y and z directions (-)
L	width of the core region along the line of measurements (m)
L_1, L_2	cross-sectional bed dimensions (m)
MCR	Maximum Continuous Rating (%)
$\dot{m}_b$	mass flow of solids in the boiler (kg/s)
$\dot{m}_m$	mass flow of solids in the cold model (kg/s)
U_0	superficial gas velocity (m/s)
U_{0b}	superficial gas velocity in the boiler (m/s)
U_{0m}	superficial gas velocity in the cold model (m/s)
U^*	dimensionless velocity, $\left(4Re_d/(3C_d)\right)^{1/3}$ (-)
u_{mf}	minimum fluidization velocity (m/s)
u_t	terminal velocity of particle (m/s)
p	pressure (Pa)
P	wetted perimeter of the cross-section (m)
PSD	particle size distribution
PA/SA	primary/secondary air ratio (-)
Re_H	Reynolds number based on the riser height H (-)
Re_p	particle Reynolds number (-)
T	temperature (K)
x	coordinate of the combustion chamber height (m)

Greek Letters

ρ_b	solids suspension density (kg/m^3)
ρ_f	gas density (kg/m^3)
ρ_p	particle density (kg/m^3)
φ	particle sphericity (-)
μ	gas viscosity (Pa s)
ε	static porosity (-)

ACKNOWLEDGEMENTS

This investigation was financially supported by the fund of statutory research of Czestochowa University of Technology. Project No:BSPB-406-301/11.

REFERENCES

Anderson, T. B., Jackson, R., A fluid mechanical description of fluidized beds. I&EC Fundam., 6, 527-539 (1967).

Bricout, V., Louge, M. Y., A verification of Glicksman's reduced scaling under conditions analogous to pressurized circulating fluidization. Chemical Engineering Science, 59, 2633-2638 (2004).

Cheng, N, -S., Comparison of formulas for drag coefficient and settling velocity of spherical particles. Powder Technology, 189(3), 395-398 (2009).

Detamore, M. S., Swanson, M. A., Frender, K. R., Hrenya, C. M., A kinetic-theory analysis of the scale-up of circulating fluidized beds. Powder Technology, 116, 190-203 (2001).

Glicksman, L. R., Fluidized bed scaleup. Chapter 13, In: Handbook of Fluidization and Fluid-Particle Systems Edited by Yang, W.-C. Marcel Dekker, New York (2003).

Glicksman, L. R., Hyre, M. R., Farrell, P. A., Dynamic similarity in fluidization. Int. J. Multiphase Flow, 20(1), 331-386 (1994).

Glicksman, L. R., Hyre, M., Woloshum, K., Simplified scaling relationships for fluidized beds. Powder Technology, 77, 177-199 (1993).

Glicksman, L. R., Hyre, M. R., Westphalen, D., Verification of scaling relations for circulating fluidized beds. Proc. of 12th Int. Conf. on Fluidized Bed Combustion, 69-80 (1993).

Glicksman, L. R., Yule, T., Dyrness, A., Carson, R., Scaling the hydrodynamics of fluidized bed combustors with cold models: Experimental confirmation. Proc. of 9th Int. Conf. on Fluidized Bed Combustors, 511-514 (1987).

Horio, M., Hydrodynamics. Chapter 2, In: Circulating Fluidized Beds, Edited by Grace, J. R., Knowlton, T. M., Avidan, A. A, Blackie Academic and Professional (1996).

Kolar, A. K., Leckner, B., Scaling of CFB boiler hydrodynamics. Proc. of the 1st National Conference on Advances in Energy Research (AER 2006), Mumbai, 34-40 (2006).

Kunii, D., Levenspiel, O., Fluidization Engineering. 2nd Ed., Butterworth-Heinemann, USA, Chapter 5 (1991).

Leckner, B., Szentannai, P., Winter, F., Scale-up of fluidized-bed combustion-A review. Fuel, 90, 2951-2964 (2011).

Mirek, P., A simplified methodology for scaling hydrodynamic data from Lagisza 460 MWe supercritical CFB boiler. Chemical and Process Engineering, 32(4/1), 245-253 (2011).

Mirek, P., Ziaja, J., The influence of sampling point on solids suspension density applied in scaling of the hydrodynamics of a supercritical CFB boiler. Chemical and Process Engineering, 32(4), 391-399 (2011).

Nowak, W., Mirek, P., Circulating fluidized bed combustion (CFBC). Chapter 16, In: Fluidized Bed Technologies for Near-Zero Emission Combustion and Gasification, Edited by F. Scala, Woodhead Publishing (2013).

Sierra, C., Bonniol, F., Occelli, R., Tadrist, L., Practical scaling considerations for dense gas fluidized beds interacting with the air-supply system. Chemical Engineering Science, 64, 3717-3720 (2009).

Sterneus, J., Johnsson, F., Leckner, B., Characteristics of gas mixing in a circulating fluidised bed. Powder Technology, 126, 28-41 (2002).

van der Meer, E. H., Thorpe, R. B., Davidson, J. F., Dimensionless groups for practicable similarity of circulating fluidized beds. Chemical Engineering Science, 54, 5369-5376 (1999).

Qi, X., Zhu, J., Huang, W., Hydrodynamic similarity in circulating fluidized bed risers. Chemical Engineering and Science, 63, 5613-5625 (2008).